Arab Journal of Physical Chemistry- http://aphyschem.org

Article/ P. N. Dave et al.

Ti-alloys Nano-catalyst for Ammonium Perchlorate thermal decomposition

Pragnesh N Dave[a*]; Pravin N Ram[a] and Shalini Chaturvedi[a]

Department of Chemistry, K.S.K.V. Kachchh University, Mundra Road, Bhuj-370 001, Gujarat, India

*Corresponding Author Email: pragneshdave@gmail.com

Received 3 December 2014,
Accepted 25 January 2015

- ## Novelty and Highlights:

1 – Synthesis of transition metal nanoalloys of Ti-Co, Ti-Ni and Ti-Zn.

2 – Studied the thermal decomposition of ammomium perchlorate over Ti-nanoalloys.

- ## Graphical Abstract:

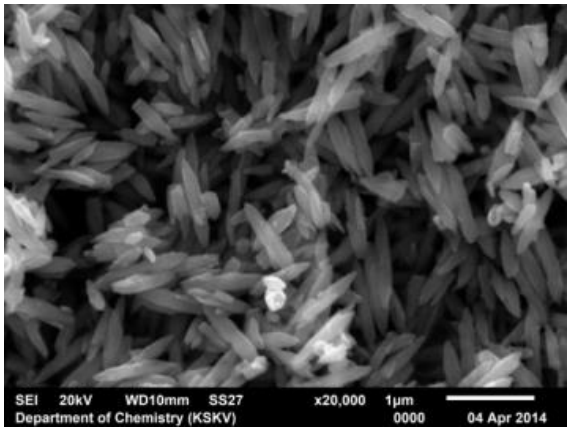

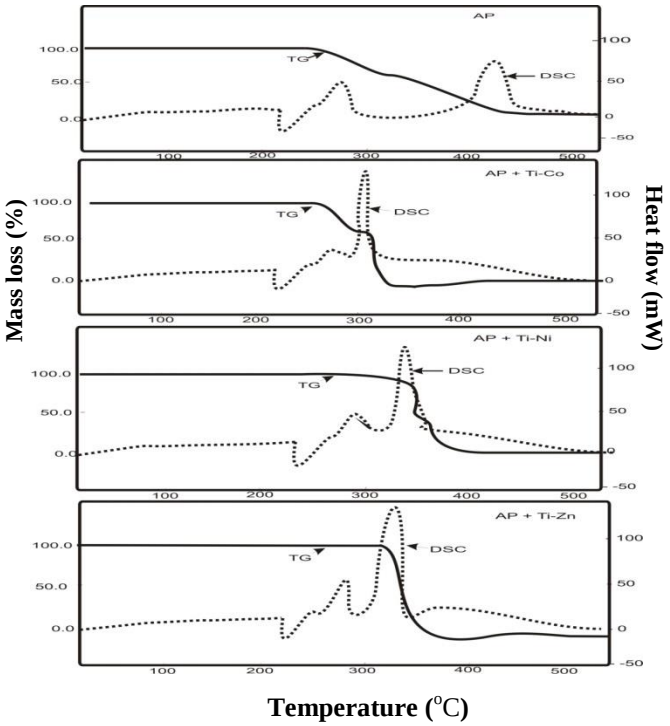

Ti-alloys nano-alloys are shows potential catalytic effect for thermal decomposition of ammonium perchlorate at much lower temperature.

Arab Journal of Physical Chemistry- http://aphyschem.org

Saudi Chemical Society

Article/ P. N. Dave et al.

Ti-alloys Nano-catalyst for Ammonium Perchlorate thermal decomposition

Pragnesh N Dave[a*]; Pravin R Ram[a] and Shalini Chaturvedi[a]

Department of Chemistry, K.S.K.V. Kachchh University, Mundra Road, Bhuj-370 001, Gujarat, India

Abstract: Transition metal nanoalloys of Ti-Co, Ti-Ni and Ti-Zn were prepared by hydrazine reduction of metal chloride in ethylene glycol at 60°C and characterized by X-ray diffraction (XRD) and Scanning electron microscopy (SEM). The average particle size for Ti-Co, Ti-Ni and Ti-Zn was measured to be 28.2, 16.1 and 24.6 respectively using X-ray diffraction pattern. The effect of bimetal nanoalloys (BMNs) on the thermal decomposition of ammonium perchlorate (AP) was investigated using Thrmogravimetric analysis (TGA), Differential Scanning Calorimetric (DSC) studies. Activation energy of high temperature decomposition (HTD) of with different alloy nanoparticles was calculated using DSC by Kissinger equation. The catalytic activity of nanoalloys is much sensitive to oxygen and may be effective to improve the decomposition efficiency of AP and AP based propellants.

Key Words: *Ammonium perchlorate (AP); TG; DSC; Activation energy; XRD*

Introduction:

An alloy is a partial or complete solid solution of one or more elements in a metallic matrix. Complete solid solution alloys give single solid phase microstructure, while partial solutions give two or more phases that may be homogeneous in distribution depending on thermal (heat treatment) history. Alloys usually have different properties from those of the component elements.

Alloying one metal with other metal(s) or non metal(s) often enhances its properties. For example, steel is stronger than iron, its primary element. The physical properties, such as density, reactivity, Young's modulus, and electrical and thermal conductivity, of an alloy may not differ greatly from those of its elements, but engineering properties, such as tensile strength [1] and shear strength may be substantially different from those of the constituent materials. This is sometimes due to the sizes of the atoms in the alloy, since larger atoms exert a compressive force on neighbouring atoms, and smaller atoms exert a tensile force on their neighbours, helping the alloy resist deformation. Sometimes alloys may exhibit marked differences in behaviour even when small amounts of one element occur. For example, impurities in semi-conducting ferromagnetic alloys lead to different properties, as first predicted by White, Hogan, Suhl, Tian Abrie and Nakamura [1-3]. Some alloys are made by melting and mixing two or more metals. Bronze, an alloy of copper and tin, was the first alloy discovered, during the prehistoric period now known as the Bronze Age; it was harder than pure copper and originally used to make tools and weapons, but was later superseded by metals and alloys with better properties. In later times bronze has been used for ornaments, bells, statues, and bearings. Brass is an alloy made from copper and zinc.

Unlike pure metals, most alloys do not have a single melting point, but a melting range in which the material is a mixture of solid and liquid phases. The temperature at which melting begins is called the solidus, and the temperature when melting is just complete is called the liquidus. However, for most alloys there are a particular proportion of constituents (in rare cases two)—the eutectic mixture—which gives the alloy a unique melting point [3].

Catalysis is the most important chemical application of metal nanoparticles and has been extensively studied. Transition metals, especially precious metals, show very high catalytic abilities for many reactions [4-6]. Nowadays bimetallic nanoparticles have been intensively for catalysis,

In material science, the range of properties of metallic systems can be greatly extended by taking mixtures of elements to generate intermetallic compounds and alloys [7]. The rich diversity of compositions, structures and properties of metallic alloys has led to widespread applications in electronic and catalysis. To fabricate materials with well defined, controllable properties and structures on the nanometre scale, afforded by intermetallic materials have generated interest in bimetallic nanoalloys. Surface structures, composition and segregation properties of nanoalloys are of interest as they are important in

determining chemical reactivity especially the catalytic activity. Moreover, nanoalloys are also of interest as they may display structures and properties which are distinct from those of the pure elemental cluster and bulk alloys. Nanoalloys have been prepared by low temperature synthetic pathway, co-decomposition, co-reduction methods etc [7].

Among the properties of metal nanoparticles, catalysis of great interest is the particle size which can affect not only the activity but also the selectivity of catalysts. Bimetallic nanoparticles, composed of two different metal elements, are of greater interest than monometallic ones, from both the scientific and technological views, for the improvement of the catalytic properties of metal particles [4-6]. This is because bimetallization can improve catalytic properties of the original single-metal catalysts and create a new property, which may not be achieved by monometallic catalysts. These effects of the added metal component can often be explained in terms of an ensemble and/or a ligand effect in catalysis have been intensively investigated, that is, .bimetallic nanoparticles. In fact, bimetallic (or multimetallic) catalysts have long been valuable for in-depth investigations of the relationship between catalytic activity and catalyst particle structure [8-11].

The ability to design the size and composition of metal particles at the nanoscale lead to improved catalytic properties. Transition metals are widely used because they possess good catalytic, electronic and magnetic properties. Investigations have indicated when metal was associated with another metal in alloy form, the properties of resulting material could be enhanced with respect to those of pure metals [12].

Composite solid rocket propellants are the major source of chemical energy in space vehicles and missiles. Ammonium perchlorate (AP) is widely used as an oxidiser in composite solid propellants [13-17]. The ballistics of a composite propellant can be improved by adding a catalyst such as ferric oxide (Fe_2O_3), copper oxide (CuO), copper chromite ($CuO.Cr_2O_3$), nickel oxide (NiO), etc, which accelerates the rate of decomposition of AP [13-17]. Recent investigations have shown that nanoparticles of transition metal oxides, without any agglomeration can increase the burning rate [18]. The efficiency of catalytic action increases sharply in nanosize oxide particles than micro scale oxide particles [19]. The size distribution, morphology and nanostructure of particles are very important characteristics and do affect the kinetics of decomposition of ammonium perchlorate.

In the present work, bi-metal nanoparticles (BMNs) of Ti with Cu, Zn and Ni are prepared by hydrazine reduction of mixture metal chloride in ethylene glycol without use of any protective agent [20]. The size of the nanoparticles was characterized by SEM and X-ray diffraction (XRD). The catalytic effect of BMNs on the thermal decomposition of AP was studied and found to be better catalyst for the AP based composite solid rocket propellants [6]. In the DSC measurement at different heating rate; mechanism of reaction will not differ because reaction rate is only dependent on temperature mechanism and independent from heating rate of sample [21].

Experimental

AP (Qualigens) was used without further purification. Crystals of AP were ground into fine powder using a pestle and mortar and sieved to 100-200 mesh. $NiCl_2$ (Finar), $ZnCl_2$ (Finar), $CuCl_2$ (Finar), $TiCl_2$ (Finar) Hydrazine (Qualikems), NaOH (Merck) and Ethylene glycol (Merck) were used as received.

Preparation of BMNs: All BMNs were prepared as reported earlier [20]. An appropriate amount of metal chloride (2.5-45 mM) was dissolved directly in ethylene glycol followed by addition of an appropriate amount of hydrazine (0.05-0.9 M) and of 1.0 M NaOH solution (10- 72 µL). At 60 ^oC, metal nanoparticles were formed after about 1 hr in a capped bottle with stirring. The reaction was performed in an organic solvent instead of aqueous solution, so it was relatively easy to form pure metals. Nitrogen gas was produced and bubbled up continuously during reaction which created an inert atmosphere and hence the passing extra N_2 gas was not necessary for the synthesis of pure BMNs.

Characterization: Characterization of BMNs has done using powder XRD and SEM techniques (JEOL; JSM-6510 LV) (Fig. 1, 2). X-ray diffraction (XRD) measurement were performed on the BMNs by an X-ray diffractometer (Rigaku; miniflex 600) using CuKα radiation (λ = 1.5418). The diffraction pattern is shown in Fig. 1. Particle size was calculated by applying Scherrer's equation [22]. SEM images are shown in fig.2.

TG (Fig 3) of AP and AP with BMNs (by mixing in ratio of 99:1) were recorded on the samples (~ 12 mg) using Perkin Elmer (Pyris Diamond) under nitrogen atmosphere (200ml/min) at a heating rate 10 $^oC\ min^{-1}$ using platinum crucible with pierced lid. DSC (Fig 3) of AP and AP with BMNs (by mixing in ratio of 99:1) were recorded on the samples (~ 12 mg) using Perkin Elmer (Pyris Diamond) under nitrogen atmosphere (200ml/min) at a heating rate 10 $^oC\ min^{-1}$ using platinum crucible with pierced lid. In this DSC method experiments had done in 3 heating rate β1=5, β2=10, β3=15 degree on minute. In dependent to model free; calculation of activation energy done by following Kissinger equation [23]

$$\frac{d\ln[\beta/T^2_{max}]}{d[1/T_{max}]} = \frac{(-E)}{R} \qquad (1)$$

On differentiation

$$\ln [\beta/T^2_{max}] = (-E)/RT + \text{Constant} \quad \textbf{(2)}$$

where *B*, *E*, *R* and *T* are the heating rate, activation energy, gas constant and a specific temperature, respectively. A plot of $\ln(B/T^2)$ versus $1/T$ yields an approximate straight line with a slope of $-E/R$.

Results and discussion

The XRD graph (Fig 1) of Ti-Co has no sharp peak which indicates amorphous nature of particles. XRD graph Ti-Zn and Ti-Ni particles have sharp peaks which confirms their crystalline nature which is consistence with the literatures [4]. The SEM image (Fig.2) of Ti-Ni show cluster of spikes while Ti-Zn has needled shaped, the particle size was calculated via Scherrer's equation [22]. Particle size 28.2, 16.1 and 24.6 nm was obtained for Ti-Co, Ti-Ni and Ti-Zn respectively.

The non-thermal TG thermogram for AP (Fig: 3) take place in two steps [24-26]. AP on heating first loses 25% of its mass at around 300 ^{o}C i.e. low temperature decomposition (LTD). Beyond this temperature a plateau is observed and AP loses 80% of its mass at around 450 ^{o}C i.e. high temperature decomposition (HTD). It can be seen from TG thermal curve of AP with alloys that the catalysts affects both LTD and HTD of AP. The higher percentage mass loss is observed in the thermal curves for AP-alloys mixture as compare with pure AP. Gasification of AP in presence of catalysts during HTD not only begin early, but also complete at lower temperatures.

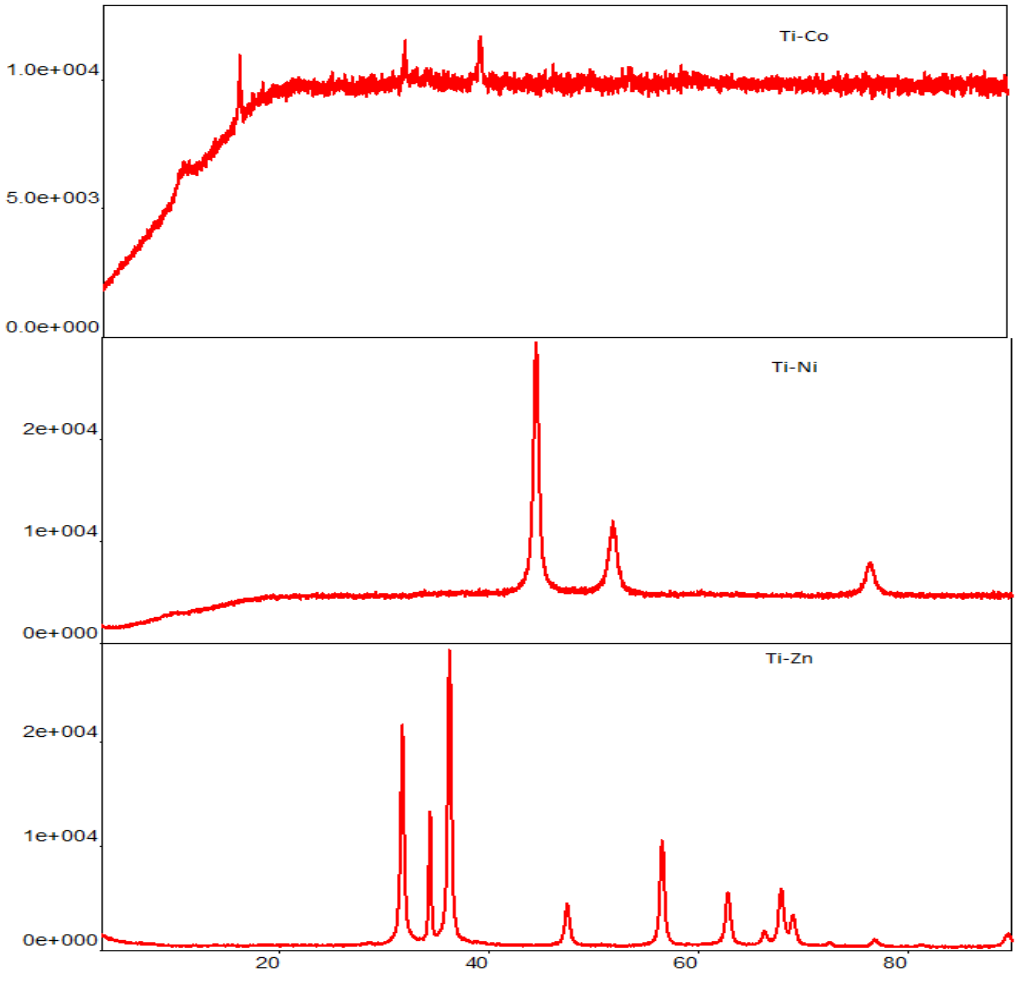

Fig. 1 XRD Pattern of Ti-alloys

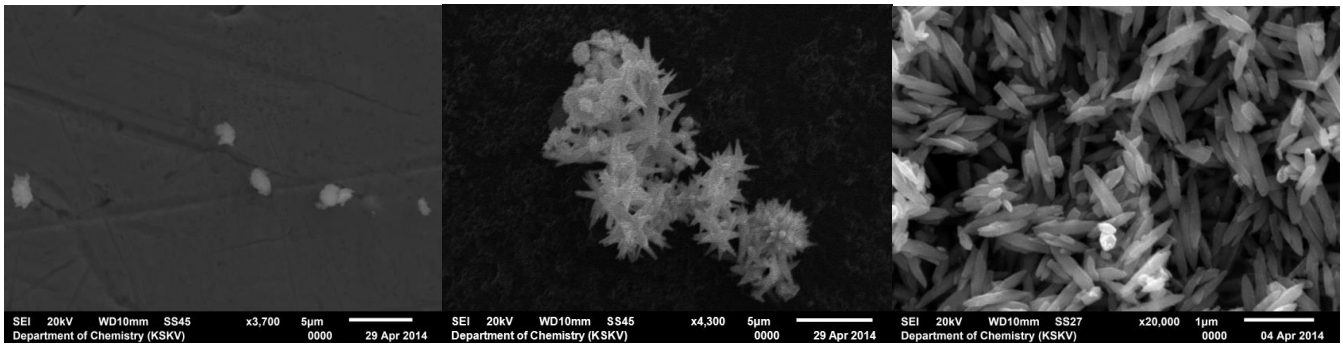

Ti-Co **Ti-Ni** **Ti-Zn**

Fig. 2 SEM image of Ti- alloys

The DSC curve as shown in Fig: 3, for pure AP shows three main events. The endothermic peak at 244 ^{o}C represents the transition from orthorhombic to cubic [27]. The thermal decomposition of AP occurs in two steps as shown in TG thermal curve of AP (Fig 3) and the first exothermic peak corresponds to LTD process and formation of intermediate product takes place. The second main exothermic peak at higher temperature (450^{0}C) corresponds to HTD process; complete decomposition of the intermediate products into volatile products [28] takes place. The DSC of AP with alloys shows a noticeable change in the decomposition pattern (Table 1). The endothermic peak shows no change in position. In contrast, there is small difference in first exothermic peak and big difference in the position of second exothermic peak. The addition of nano alloys lowers the high decomposition temperature of AP by 100-90 ^{o}C. HTD process for pure AP was observed at lower temperature for AP with alloys indicating the effect of the catalysts.

Table 1: DSC phenomenological data of the AP and AP with BMNs

	DSC	
Samples	**Peak (Temp./^{0}C)**	**Nature**
AP	285	Exo
	420	Exo
AP+Ti-Ni	290	Exo
	332	Exo
AP+Ti-Zn	275	Exo
	331	Exo
AP+Ti-Co	265	Exo
	295	Exo

$$NH_4^+ + ClO_4^- = NH_3\text{-}H\text{-}ClO_4 = NH_3\text{-}HClO_4 = NH_3\ (a) + HClO_4\ (a) = NH_3\ (g) + HClO_4(g)$$

(I) **(II)** **(III)**

The activation energy for LTD and HTD of AP and AP-nano alloys under continuous heating was calculated by Kissinger equation. A plot of $\ln(\beta/T^2_{max})$ versus $1/T$ [Fig. 4] yields an approximate straight line with a slope of $-E/R$. Calculated activation energy of AP and AP-nanoalloys at HTD has been shown in the Table 2 which clearly shows the lowing in activation energy for HTD for AP in presence of nanoalloys. Remarkable lowering has been found in presence of Ti-Co alloys.

As reported earlier nanopowder contain many defects over crystal lattice. Atoms on the defects are not saturated and tend to become steady by absorbing materials with surplus electrons onto its surface.

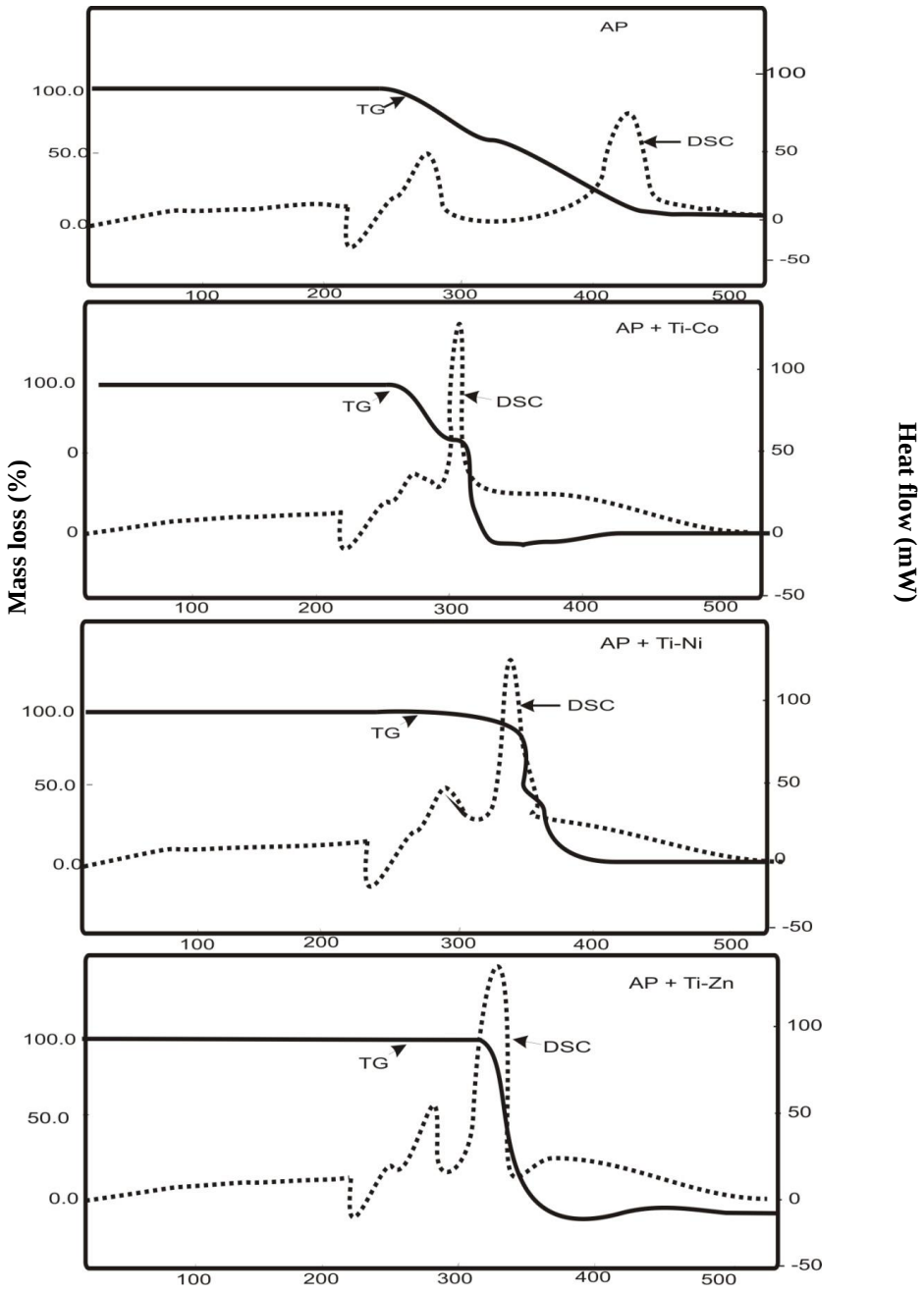

Fig. 3 TG-DSC Thermogram of AP and AP with BMNs

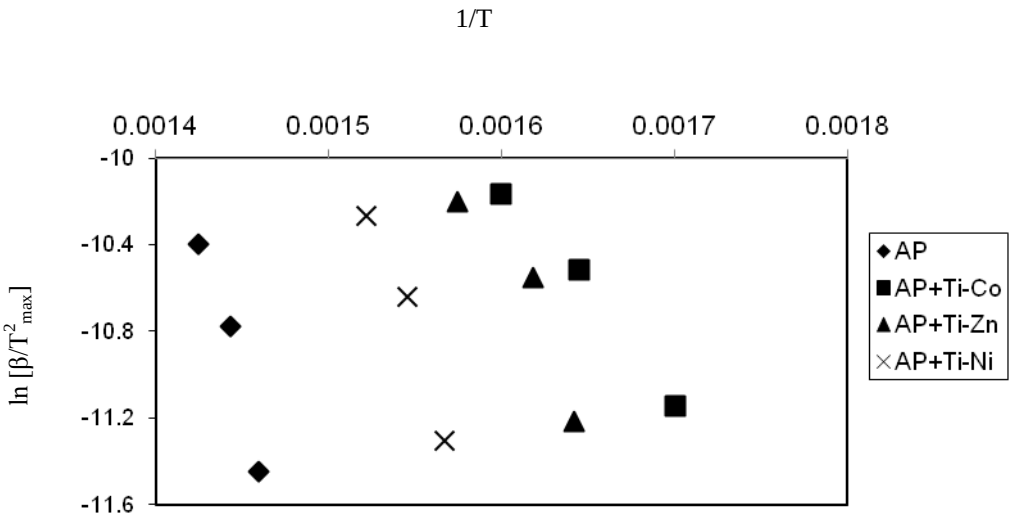

Fig. 4 Plot of ln (β/T^2_{max}) versus 1/T for AP and AP with BMNs

Table 2: Activation energy of HTD step (via Kissinger equation) of AP and AP with Ti-alloys

Sample	Activation energy (E) (kJ/mol)
AP	245.832
AP + Ti-Ni	190.657
AP+ Ti-Zn	118.617
AP+ Ti-Co	81.231

The N atom of AP contains surplus electrons, so the N–X bond becomes weak and easy to break owing to the absorbing of the N atom on the surface of metal atom. This is advantageous in the production of NH_3. It is also reported [29] that nitrogen oxides react easily with Cu:

$$4Cu + 2NO = 2Cu_2O + N_2,$$

$$2Cu_2O + 2NO = 4CuO + N_2.$$

Because the nitrogen oxides are produced both at the first and second decomposition step of AP, the nanometer Cu can accelerate the decomposition of AP by catalyzing the decomposition of nitrogen oxides. Because of both these effects, nanometer Cu powder shows high catalytic effect on the first and second decomposition step of AP.

TG-DSC thermogram result shows thermal decomposition occurs at low temperature with BMNs. Kinetic energy for thermal decomposition of AP is 245.832 kJ/mol while kinetic energy for AP with BMNs are much lower as compare to AP which are calculated via Kissinger equation (table 2). From these experimental results we can conclude these nanoalloys are better catalyst for thermal decomposition of AP and these catalysts can be use in the formation of AP-HTPB composite solid rocket propellants for better result.

According to proton transfer mechanism [25], (I) corresponds to the pair of ions in AP lattice. The breaking of an N-H bond, then proton transfer from ammonium ion to perchlorate ion to form an O-H bond leads to the formation of NH3 and HClO4 molecules is a

primary step in condense phases. Secondary reactions occur at higher temperature through complex competitive steps to produce gaseous products. It is known that the surface area of BMNs is large due to their very small size and there are many reactive sites over the surface. Thus during the second exothermic decomposition of AP, BMNs can adsorb the gaseous reactive molecules on their surface and promote the reactions.

Conclusions

BMAs (Co-Cu, Co-Zn, Co- Fe) were prepared by hydrazine reduction method, characterized by XRD, SEM and used as catalyst in the high temperature thermal decomposition of AP via TGA, DSC. The catalytic activity of nanoalloys is much sensitive to oxygen and may be effective to improve the decomposition efficiency of AP and AP based propellants.

Acknowledgements

The authors are grateful to Chemistry Department of KSKV University, Bhuj for laboratory facility and for XRD, SEM and TGA-DSC analysis.

References

1. P. Ball and L. Garwin, *Nature*, 1992, **355**, 761.
2. C. Michael Hoga, *Phys. Rev*, 1969**, 188,** 2, 870.
3. Shufen L., J. Zhi and Y. Shuqin, *Fuel Chemistry*, 2002, **47,** 2, 596.
4. Shalini Chaturvedi, Pragnesh N Dave and Nikul N Patel, *Synthesis and Reactivity in Inorganic, Metal-Organic, and Nano-Metal Chemistry*, 2014, **42**, 2, 258-262.
5. Supriya Singh, Pratibha Srivastava, Gurdip Singh, Journal of Alloys and Compounds, 2013, **562**, 150–156.
6. Shalini Chaturvedi & Pragnesh N Dave; *J. of saudia Chemical society*; 2013, **17**, 135-149.
7. R. Ferrando, J. Jellinek and R. L. Johnston, *Chem. Rev.*, 2008, **108**, 3, 845.
8. L. N. Lewis, *Chem. Rev.*, 1993, **93**, 2693.
9. G. Schmid, in *Clusters and Colloids*, VCH, Weinheim, 1994.
10. H. Bo. nnemann, W. Brijoux, R. Brinkmann, E. Dinjus, T. Jouben and B. Korall, *Angew. Chem., Int. Ed. Engl*., 1991, **30**, 1312.
11. Naoki Toshima and Tetsu Yonezawa, *New J. Chem.*, 1998, 1179-1201.
12. Shalini Chaturvedi & P.N. Dave; *J. Of Material Science*; 2013, **48**, 3605-3622.
13. S.M. Shen; S.I. Chen, & B.B.Wu, *Thermochim Acta*, 1993, **223**, 135-43.
14. A.A Said , *Thermal Analysis*, 1991, **37**, 959-62 .
15. A.K. Nema; S. Jain; S. K. Sharma; S. K. Nema & S. K. Verma, *Int. J. Plastics Tech*., 2004, **8**, 344-54.
16. J. Gao, F. Guan. F & Y. Zhao, *Mat. Chem. Phys*., 2001, **71**, 215-219.
17. S. Chaturvedi and P N Dave, *J. of Exp. Nanosci*.; 2011, 1-27.
18. V N Simonenko; V E Zarko; A B Kiskin, & V S Sedoi, *In* 32nd International Annual conference of ICT, 2001, 122/1.
19. MM Telkar; CV Rode; RV Choudhary; SS Joshi, & AM Nalawade, *J. Appl. Cata., A*, 2004, **273**, 11-19.
20. SH Wu and DH Chen, *Journal of Colloid and Interface Sci.*, 2003, 59, 282–286.
21. Wang Huan-Rong, Ye Yi-Fu, Min Guang-Hui, Chen Ying , Teng Xin-Ying; *Journal of Alloys and Compounds*, 2003, **353**, 200–206.
22. LS Birks and H Friedman, *J. Appl, Phys*, 1946, **17**, 687-692.
23. K Lu, W.D. Wei, J.T.Wang, *J. Appl. Phys*.; 1991, **69**, 7345-7347.
24. LL Bircumshaw and BH Newmann, The thermal decomposition of ammonium perchlorate I. Introduction, experimental, analysis of gaseous products, and thermal decomposition experiments; Proc. Roy. Soc.; A, 1954, **227**, 115-132.
24. PMW Jacobs and GS Parasone, Combust. Flame; 1969, **13**, 419-425.
25. WA Rosser and SH Inami; *Combust. Flame*; 1968, **12**, 427-435.
26. K Kishore and K Sridhara, Solid propellant chemistry: condensed phase behaviour of ammonium perchlorate based solid propellants, *DESIDOC*, New Delhi, 1990, 10.
27. J. Zhi, Z. Feng-Qi, *J. Propul. Tech.* 2002, **23,** 258-261.
VV Boldyrev, Thermochim*Acta*, 2006, **443**, 1-36.